Detection and Localization of Prostate Cancer: Correlation of ^{11}C-Choline PET/CT with Histopathologic Step-Section Analysis

Mohsen Farsad, MD[1]; Riccardo Schiavina, MD[2]; Paolo Castellucci, MD[1]; Cristina Nanni, MD[1]; Barbara Corti, MD[3]; Giuseppe Martorana, MD[2]; Romeo Canini, MD[4]; Walter Grigioni, MD[3]; Stefano Boschi, ScD[1]; Mario Marengo, ScD[1]; Cinzia Pettinato, ScD[1]; Eugenio Salizzoni, MD[4]; Nino Monetti, MD[1]; Roberto Franchi, MD[1]; and Stefano Fanti, MD[1]

[1]Nuclear Medicine Department, PET Unit, Policlinico S. Orsola-Malpighi, Bologna, Italy; [2]Urology Department, Università di Bologna, Bologna, Italy; [3]Pathology Department, Università di Bologna, Bologna, Italy; and [4]Radiology Department, Università di Bologna, Bologna, Italy

This study evaluated the potential usefulness of ^{11}C-choline PET/CT for detection and localization of tumors within the prostate. We used the results of step-section histopathologic examination as the standard of reference. **Methods:** The results were analyzed on a sextant basis. We reviewed the results of the ^{11}C-choline PET/CT scans of 36 patients with prostate cancer and of 5 control subjects with bladder cancer. All patients underwent ^{11}C-choline PET/CT and, subsequently, radical prostatectomy with lymph node dissection within 1 mo. ^{11}C-Choline PET/CT scans were obtained 5–10 min after intravenous injection of 370–555 MBq of ^{11}C-choline. Images were reviewed visually and semiquantitatively using maximum SUV and tumor-to-background ratio. **Results:** On a sextant basis, histopathologic analysis detected cancer foci in 143 of 216 sextants; high-grade prostate intraepithelial neoplasm foci were detected in 89 of 216 sextants (in 59 sextants in association with carcinoma, in 30 sextants alone), acute prostatitis was detected in 7 of 216 sextants (in 3 sextants in association with carcinoma, in 4 sextants alone), and 39 of 216 sextants were normal. PET/CT demonstrated focal ^{11}C-choline uptake in 108 sextants (94 of which involved tumor), and 108 sextants showed no abnormal ^{11}C-choline uptake (49 of which were false negative). The sensitivity, specificity, accuracy, positive predictive value, and negative predictive value of PET/CT were 66%, 81%, 71%, 87%, and 55%, respectively. In the 5 control subjects, high-grade prostate intraepithelial neoplasm was detected at histologic examination in 16 of 30 sextants. PET/CT showed increased ^{11}C-choline uptake in 5 of 16 sextants. **Conclusion:** This study demonstrated the feasibility of using ^{11}C-choline PET/CT to identify cancer foci within the prostate. However, we also found that ^{11}C-choline PET/CT has a relative high rate of false-negative results on a sextant basis and that prostatic disorders other than cancer may accumulate ^{11}C-choline. Therefore, our data do not support the routine use of PET/CT with ^{11}C-choline as a first-line screening procedure for prostate cancer in men at high risk.

Key Words: ^{11}C-choline PET/CT; prostate cancer; tumor localization; radionuclide imaging

J Nucl Med 2005; 46:1642–1649

Received Apr. 19, 2005; revision accepted Jun. 27, 2005.
For correspondence or reprints contact: Stefano Fanti, MD, Medicina Nucleare, Policlinico S. Orsola Malpigli, Via Massarenti, 40100 Bologna, Italy.
E-mail: fanti@aosp.bo.it

Early detection of prostate cancer may feasibly lead to an increased cure rate (*1–4*). Biopsy guided by transrectal ultrasound (TRUS) represents the standard method for detecting prostate cancer. Unfortunately, the false-negative rate of TRUS-guided biopsy is high (30%–40%), and biopsy must often be repeated (*5–7*). In this scenario, it is reasonable to look for other imaging techniques able to reveal prostate cancer. Of all available imaging modalities, metabolic diagnostic methods seem to be most promising. MRI with an endorectal coil shows good accuracy in local staging (*8*) of prostate cancer and is more accurate than TRUS in tumor detection but lacks specificity (benign conditions such as prostatitis, postbiopsy bleeding, or scarring can mimic cancer) (*9*). Recent studies have demonstrated that MRI spectroscopic evaluation of citrate and choline metabolism improves the specificity of this diagnostic method (*10,11*). This technology remains in evolution, and continued advances in accuracy and use are expected.

PET using different positron-emitting radiopharmaceuticals has emerged as a promising new metabolic diagnostic tool for evaluation of a variety of malignant diseases, including prostate cancer (*12–17*). In recent years, the use of ^{11}C-choline in PET studies has been introduced for identification of prostate tumors (*18*). ^{11}C-Choline is a precursor of the biosynthesis of phosphatidylcholine, which is a major phospholipid in the cell membrane. Various studies have revealed that malignant tumors induce high levels of choline kinase activity, resulting in increased levels of membrane phospholipids (*18–22*). It has been hypothesized that uptake of ^{11}C-choline reflects proliferative activity by estimating membrane lipid synthesis (*20*). However, a recent study found that radiolabeled choline uptake does not correlate with cell proliferation in prostate cancer (*23*). Thus, the exact uptake mechanism has to be established. ^{11}C-Choline PET has been proposed for the imaging of recurrent prostate cancer and has demonstrated promising results (*18,19*). As yet, no agreement exists as to the value of PET in localization of early prostate cancer, and recent reports on this issue

have been contradictory. Some authors postulated a significant overlap in uptake values of ^{11}C-choline between prostate cancer and benign prostate hyperplasia (*20*), whereas others demonstrated that ^{11}C-choline PET was effective in revealing prostate cancer within the gland (*21*). Various causes may account for the heterogeneity in diagnostic performance: differences in patient population, differences in study methodology, and application of PET scanners instead of new-generation PET/CT scanners. To our knowledge, no study has correlated PET/CT findings with histopathologic analysis of the whole prostate on a sextant basis.

The aim of this study was to evaluate the potential usefulness of ^{11}C-choline PET/CT for detection and localization of tumors within the prostate. We used the results of a step-section histopathologic examination as the standard of reference.

MATERIALS AND METHODS

We retrospectively reviewed the PET/CT results for 36 patients (mean age, 63.4 y; range, 51–75 y; mean preoperative prostate-specific antigen [PSA] level, 12.3 ng/mL; range, 2–70 ng/mL) with biopsy-proven prostate cancer, who subsequently underwent, within 1 mo, videolaparoscopic or retropubic radical prostatectomy with pelvic lymph node dissection. The study was performed in line with the Helsinki declaration and national regulations. All patients provided informed consent for participation and anonymous publication of data.

^{11}C-Choline PET/CT was performed before prostate biopsy to avoid possible postbiopsy effects on the PET/CT results. Prostate biopsy was indicated if total PSA was >10 ng/mL; if total PSA was 4–10 ng/mL, with <13% free PSA or a PSA velocity of >0.75 ng/mL/y; if the findings of digital rectal examination (DRE) were abnormal, or if a hypoechoic lesion suggestive of prostate cancer was found on TRUS.

Patients were excluded from the study if they had proven concomitant cancer other than prostate cancer (except for the control group, which had bladder cancer) or had been treated with 5-α-reductase inhibitors before PET/CT (to obviate possible metabolic effects of these drugs on prostate metabolism and ^{11}C-choline uptake).

TRUS-guided biopsy was performed according to a 12-core systematic biopsy scheme (standard sextant scheme plus laterally directed biopsies at the prostate apex, mid, and base) (*24*); all patients but 3 underwent only 1 set of biopsies. Extra cores were obtained in suggestive regions on DRE, hypoechoic areas, areas of focal ^{11}C-choline uptake on PET/CT (in only 3 patients at repeated biopsy), and in glands larger than 50 cm^3. Every core was placed into a container, labeled, and reviewed at a central pathology laboratory.

Thirty-three patients showed results positive for cancer at the first biopsy, and 3 patients (patients 12, 34, and 36) at repeated biopsies; all patients underwent radical prostatectomy within 1 mo. After surgical prostate resection, careful histologic evaluation was performed. After coating with india ink and fixation in 10% buffered formalin, axial step sections were obtained at 4- to 5-mm intervals transversely in a plane perpendicular to the long axis of the gland. The prostate gland was divided into sextants: right apex (Ra), right middle (Rm), right base (Rb), left apex (La), left middle (Lm), and left base (Lb). The base was defined as the upper third of the prostate, extending from the bladder margin; the mid region was defined as the central third; and the apex was defined as the remaining inferior third. The presence and location of cancer foci, high-grade prostate intraepithelial neoplasm (HGPIN), acute prostatitis, and benign prostate hyperplasia were determined by 2 independent pathologists for each sextant. Each tumor was staged according to the 2002 TNM classification of the International Union Against Cancer, and cell differentiation was assessed according to the Gleason score.

The patient characteristics, pathologic stage and grade of the tumor, PSA value, and prostate volume are shown in Table 1.

We performed ^{11}C-choline PET/CT on a control group of 5 patients (mean age, 67 y; range, 64–71 y) with infiltrating transitional bladder carcinoma who underwent radical cystoprostatovesiculectomy (Table 2); inclusion criteria were PSA < 4 ng/mL and no suggestion of prostate cancer on DRE and TRUS. Prostate biopsy was not performed on these patients, but histopathologic examination of a whole-mount section of prostate was performed and the results of PET/CT reviewed.

Radiopharmaceuticals

^{11}C-Choline was synthesized according to the solid-phase method, essentially as described by Pascali et al. (*25*), in a modified commercial synthesis module (TRACERlab; GE Healthcare). $^{11}CO_2$ produced by a PETtrace cyclotron (GE Healthcare) was converted into $^{11}CH_3I$ by the conventional $LiAlH_4$/HI reaction. $^{11}CH_3I$ was used for the N-methylation of dimethylaminoethanol (60 μL) placed directly on a solid-phase support (C18 SepPak Light; Waters). After a washing step with ethanol and water, ^{11}C-choline retained on a cation exchange resin (SepPak Accell Plus CM; Waters) was eluted with saline, sterilized by a 0.22-μm filter, and collected in a final volume of 8 mL.

Radiochemical purity was evaluated by means of a high-performance liquid chromatography radiodetector equipped with a reversed-phase column, and the concentration of organic solvents was measured by gas chromatography. Endotoxin content was measured by the conventional lysosomal acid lipase method (Cambrex Bioscience).

PET/CT

All PET scans were obtained with the Discovery LS (GE Healthcare), a dedicated PET/CT scanner comprising an ADVANCE Nxi PET scanner and a LightSpeed DS multislice CT tomograph. The patients fasted at least 6 h before the PET acquisition and received an intravenous injection of 370–555 MBq of ^{11}C-choline. Starting 5 min after injection (according to the ^{11}C-choline kinetics results of previous papers (*18,20*)), emission data were acquired at 2–3 bed positions (the ADVANCE has 15 cm of axial field of view) from the upper pelvis through the mid thigh for 5 min at each position. The parameters of the multidetector helical CT scan were 140 kV, 80 mA, 0.8 s per tube rotation, slice thickness of 5 mm, pitch of 6, and table speed of 22.5 mm/s. CT images were used for both attenuation correction of emission data and image fusion.

Image Analysis

All PET images were analyzed with dedicated software (eNTEGRA; GE Healthcare) that allowed review of PET, CT, and fused-image data.

PET images were first assessed visually, using transaxial, sagittal, and coronal displays. Any abnormal focus of increased

TABLE 1
Clinical Characteristics of Patients with Prostate Cancer

Patient no.	Age (y)	PSA (ng/mL)	Free-to-total PSA	DRE	Hypoechogenic lesion on TRUS	Prostate volume (cm^3)	No. of biopsy cores	Treatment	TNM	Gleason score
1	65	9	11	−	+	70	14	RRP	T2c N0	Gs4+3
2	60	3	15	+	+	30	12	RRP	T3a N0	Gs3+4
3	56	6.4	12	−	−	25	13	VLRP	T3a N0	Gs3+3
4	60	9	13	−	−	75	10	VLRP	T2c N0	Gs3+4
5	65	15	9	−	−	45	12	RRP	T2c N0	Gs3+3
6	63	5	20	−	−	50	12	VLRP	T2c N0	Gs1+1
7	61	5	28	−	+	75	12	RRP	T3a N0	Gs4+3
8	57	13	11	−	−	60	12	VLRP	T3a N0	Gs3+3
9	64	2	7	−	−	25	12	VLRP	T2a N0	Gs2+1
10	69	9	2	+	+	35	13	RRP	T3a N0	Gs3+3
11	68	9	7	−	−	50	12	RRP	T2c N0	Gs3+3
12	70	28	13	−	−	50	18	RRP	T2c N0	Gs3+3
13	57	8	12	−	−	50	12	VLRP	T2c N0	Gs2+3
14	62	7	8	−	−	35	15	RRP	T2c N0	Gs3+1
15	51	10	11	+	+	40	12	VLRP	T3a N0	Gs3+3
16	75	8	7	+	+	40	12	RRP	T2c N1	Gs3+3
17	72	10	20	+	+	55	12	RRP	T2c N0	Gs2+3
18	64	21	16	−	+	35	12	VLRP	T3a N0	Gs3+4
19	58	5	9	−	+	50	12	RRP	T3a N0	Gs3+3
20	72	10	8	+	+	30	12	VLRP	T3a N0	Gs4+3
21	68	20	13	+	+	20	10	RRP	T3a N0	Gs3+3
22	60	8	9	−	−	30	12	RRP	T3a N0	Gs3+2
23	63	5	19	+	+	40	15	VLRP	T2b N0	Gs3+3
24	72	70	18	+	+	50	10	RRP	T3b N1	Gs4+3
25	63	7	13	+	+	30	10	RRP	T3b N1	Gs4+3
26	59	12	7	−	−	50	12	VLRP	T2c N0	Gs3+3
27	70	59	15	−	+	70	14	RRP	T2c N0	Gs3+2
28	65	5	7	−	−	50	13	RRP	T3a N0	Gs3+3
29	60	5	6	−	−	30	12	RRP	T2c N0	Gs3+3
30	68	7	9	−	−	30	12	RRP	T2c N0	Gs3+3
31	58	5	7	+	+	25	12	RRP	T3b N0	Gs4+3
32	51	12	11	+	+	50	12	RRP	T3b N1	Gs4+3
33	69	6.2	10	−	−	50	12	RRP	T2c N0	Gs2+2
34	71	17	13	−	−	30	15	RRP	T3a N0	Gs3+3
35	65	7	12	+	+	40	12	RRP	T3a N0	Gs3+3
36	52	5.2	8	−	−	40	12	RRP	T2c N0	Gs3+3

RRP = radical retropubic prostatectomy; VLRP = videolaparoscopic prostatectomy.

^{11}C-choline uptake in the prostate gland was identified by 2 experienced, independent nuclear medicine physicians unaware of the clinical data. To allow an objective assessment of the amount of tracer uptake, we evaluated the ^{11}C-choline uptake by semiquantitative analysis using the maximum standardized uptake value (SUVmax) and the tumor-to-background (T/B) ratio for each abnormal focus. Background activity was considered the uptake of 4 small (5-mm) regions of interest in the sextants without pathologic uptake or in areas showing the lowest activity. PET/CT findings were compared with histopathologic results on a sextant basis. To determine the exact location of intraprostatic focal uptake, we used an integrated PET/CT system. Sextants were defined using the same criteria as for histopathologic evaluation.

TABLE 2
Clinical Characteristics of Control Group with Infiltrating Transitional Bladder Carcinoma

Patient no.	Age (y)	PSA (ng/mL)	Free-to-total PSA	DRE	TRUS	Prostate volume (cm^3)	TNM (bladder)	Tumor grade
1	65	2.1	18	−	−	30	T1 N0	2–3
2	70	2.8	24	−	−	40	T3b N0	3
3	65	2.0	20	−	−	30	T1 N0	3
4	64	1.3	30	−	−	45	T1 N0	3
5	71	1.6	25	−	−	40	T3b N0	3

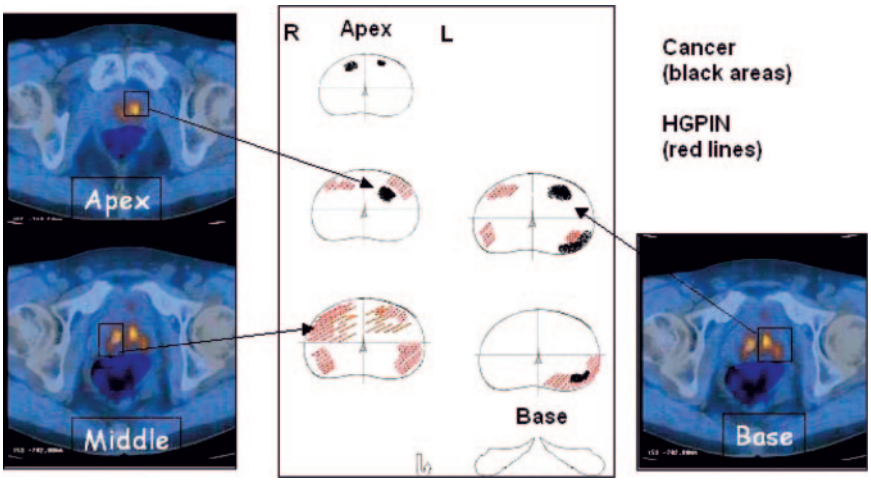

FIGURE 1. PET/CT results and histologic matching.

One of the authors who did not read the PET/CT scans or perform the pathologic examinations entered all PET findings and histopathologic results on a section-by-section basis on standardized data forms with diagrams (Fig. 1). These diagrams were used to match and compare the sites of pathologic findings. For a correct localization and matching of pathologic results, the use of an integrated PET/CT system, rather than PET alone, was essential (*26,27*). For statistical evaluations, the tumor site on PET/CT images was considered to match the histopathologic site if the tumor was present in the same sextant of the prostate within a range of 1 section. In addition, the tumor had to be in the same anterior or posterior location.

Statistical Analysis

Descriptive statistics included sensitivity, specificity, accuracy, and positive and negative predictive values of PET/CT for sextant localization of prostate cancer. Possible correlation between PSA, Gleason grade, Gleason score, and SUVmax were investigated for linear correlation (R^2 test).

RESULTS

Sextant-per-sextant step-section histology confirmed multifocal stage T2 or T3 prostate cancer in all 36 patients, with a mean Gleason score of 5.9 (range, 2–7). On a sextant basis, histopathologic analysis identified cancer foci in 143 of 216 sextants, HGPIN foci in 89 (in 59 sextants in association with carcinoma, in 30 sextants alone), acute prostatitis foci in 7 (in 3 sextants in association with carcinoma, in 4 sextants alone), and normal tissue or benign hyperplasia in 39. Because of the diffuse and constant presence of benign hyperplasia in almost all prostatic regions, no distinct analysis could be performed.

PET/CT visual analysis identified in almost all patients 1 focus of abnormal ^{11}C-choline uptake. However, in 1 patient (patient 7) PET/CT demonstrated an abnormal focal accumulation only in the area involved by HGPIN and found negative results for tumor in the contralateral region: Overall, at least 1 primary prostatic tumor focus could correctly be visualized through PET/CT in a total of 35 of 36 patients.

On a sextant basis, PET/CT demonstrated focal ^{11}C-choline uptake in 108 sextants (50%): Histologic examination showed that 94 of 108 were affected by tumor (Fig. 2), 10 by HGPIN, 2 by HGPIN and acute prostatitis, and 2 by benign prostate hyperplasia or no pathologic finding. In sextants with areas of abnormal ^{11}C-choline uptake, the mean SUVmax was 5.3 ± 2.2 (range, 2.2–12) and the mean T/B ratio was 2.0 ± 0.5 (range, 1–3.4).

Among all true-positive foci of abnormal ^{11}C-choline uptake, 52 of 94 were affected by tumor alone (mean SUVmax, 5.4 ± 1.9; range, 2.5–8.4), 34 by tumor and HGPIN (mean SUVmax, 4.5 ± 2.1; range, 2.2–10), 3 by tumor and prostatitis (mean SUVmax, 4.0 ± 2.3; range, 1.9–8.4), and 5 by tumor and both HGPIN and prostatitis

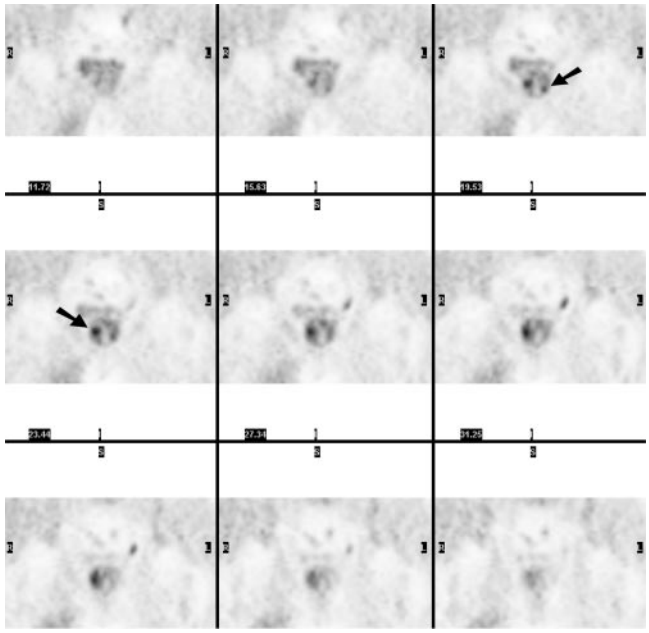

FIGURE 2. Patient 6: Coronal PET images show 2 foci of pathologic uptake in left and right mid regions (arrows), confirmed to be the only foci of cancer on histologic examination.

TABLE 3
Biopsy, PET, and Histologic Results on Sextant Basis

Patient no.	Biopsy	PET SUVmax	Background SUV	Carcinoma	HGPIN
1	La, Lm	Rm, 4.9; La, 4	2.5	Ra, Rm, La, Lm	
2	Ra, Rm, Rb, La, Lm, Lb	Ra, 2.9; Rm, 2.9; La, 2.5	1.5	Ra, Rm, Rb, La, Lm, Lb	
3	Lb	Rm, 8.4; Lm, 6.1; Lb, 6.1	4.0	Lm, Lb	Rm, Rb
4	Rm	Ra, 3.3; Rm, 3	2.0	Ra, Rm, La, Lb	Rm, Rb, Lm, Lb
5	Ra, Rb	Ra, 5.4; Rm, 8.1; Rb, 8.1; Lm, 4.3; Lb, 4.5	2.9	Ra, Rm, Rb, La, Lm, Lb	Lb
6	Lm	Rm, 7.4; Lm, 6.4	3.0	Rm, Lm	Rm, Lm
7	Lm, Lb	Rm, 4.9; Rb, 5.7	2.0	Lm, Lb	Rm, Rb, Lm, Lb
8	Rb, Rm, Lm, Lb	Rm, 4.3; Rb, 5.3; La, 4.4; Lm, 4.2; Lb, 4.5	2.5	Rm, Rb, La, Lm, Lb	Rm, Rb, Lb
9	Rm	Rm, 4.6; Rb, 4.6	2.4	Rm, Rb	Rb, Lb
10	Rb	Rm, 6.4; Rb, 5.5; Lm, 5	2.7	Rm, Rb	Lm, Lb
11	Rm	Rm, 2.9; Lm, 2.8	1.8	Rm, Lm	
12	Rm,* Lm*	Ra, 8.4; Rm, 8.4; Rb, 8.4; Lm, 7.8; Lb, 7.8	2.5	Ra, Rm, Rb, Lm, Lb	
13	Rb	Rm, 5.5; Rb, 5.5	3.0	Rm, Rb, Lb	Rm, Rb, Lm, Lb
14	La, Lm	Rm, 4; Lm, 4.7	2.8	Ra, La, Lm, Lb	Rm, Rb, Lm, Lb
15	Ra, Rm	Ra, 4.3; La, 4.3	2.5	Ra, Rm, La	Rm
16	Lm, Lb	Rm, 3; Lm, 3; Lb, 3.2	2.0	Rm, Lm, Lb	Rm, Rb, Lm, Lb
17	La, Lb	Rm, 4.9; Rb, 4.9; Lm, 4.9; Lb, 4.9	2.5	Rm, Rb, Lm, Lb	Rm, Rb, Lm, Lb
18	Rm	Rm, 4.1; Rb, 4.4	2.3	Ra, Rm, Rb	Rm, Lb
19	La, Lm	Rm, 2.8; La, 3; Lm, 3; Lb, 3.1	1.9	Rm, La, Lm, Lb	Ra, Rm, Rb, La, Lm, Lb
20	Ra, Rm, Rb, Lb	Ra, 2.7; Rm, 2.7; Rb, 2.8	1.4	Ra, Rm, Rb, Lb	Rm, Rb, Lm, Lb
21	Rm, Rb, Lb	Ra, 4.9; Lm, 7; Lb, 7	3.0	Ra, Rm, Rb, La, Lm, Lb	Rm, Rb, Lm, Lb
22	La, Lm, Lb	Rb, 4.3; Lm, 5; Lb, 5	2.3	La, Lm, Lb	Rm, Rb
23	Lm, Lb	Rm, 4.5	2.2	La, Lm, Lb	Rm, Lm, Lb
24	Ra, Rm, Rb, La, Lm, Lb	Rm, 7; Rb, 7; Lm, 5.9	3.3	Ra, Rm, Rb, La, Lm, Lb	
25	Rm, Rb, La, Lm, Lb	Lm, 4.1; Lb, 3.2	2.0	Ra, Rm, Rb, La, Lm, Lb	
26	La	Ra, 4.6; La, 5.7; Lm, 5	2.4	Ra, Rm, La, Lm, Lb	Lb
27	Rm, Lm	Rm, 7.8; Rb, 7.8; La, 5.7; Lm, 5.7	3.0	Ra, Rm, Rb, La, Lm, Lb	Ra, La, Lb
28	Lm, Lb	Ra, 12; Rm, 12; Rb, 12; La, 10; Lm, 10; Lb, 10	5.0	Lm, Lb	Rm, Rb, La, Lm, Lb
29	Ra, Rb, La, Lm, Lb	Rb, 2.2; Lb, 2.2	1.6	Ra, Rb, Lm, Lb	Rm, La, Lm
30	Rm, Lm, Lb	Lm, 2.2	1.1	Rm, Lm, Lb	Rm, Rb, Lm, Lb
31	Ra, Rm, La, Lm	Rm, 5.8; Lm, 8.5; Lb, 8.5	2.8	Ra, Rm, La, Lm, Lb	
32	Ra, Rm, Rb, La, Lm, Lb	Rb, 3.3; Lm, 2.9	2.0	Ra, Rm, Rb, La, Lm, Lb	Rb
33	Lm, Lb	Ra, 5.3; Rm, 5.3; La, 5.3; Lm, 5.3; Lb, 5.3	3.0	Ra, Rm, Rb, Lm, Lb	Rb, Lb
34	Ra,* Rm,* La,* Lm*	Ra, 4; Rm, 6.6; La, 6.6; Lm, 4	2.0	Ra, Rm, La, Lm, Lb	
35	Rm, Lm, Lb	Rm, 5.6; Rb, 5.4; Lm, 6.9; Lb, 6.2	2.8	Rm, La, Lb	Ra, Rm, Rb, La, Lm, Lb
36	Rb,* La,* Lm,* Lb*	Rb, 4.6; La, 3.2; Lm, 4; Lb, 4.6	2.2	Rb, La, Lm, Lb	Ra, Rm, Rb, La, Lm, Lb

*Positive on repeated biopsy.
La = left apex; Lb = left base; Lm = left middle; Ra = right apex; Rb = right base; Rm = right middle.

(mean SUVmax, 4.9 ± 2.3; range, 2.1–10). PET/CT demonstrated pathologic uptake in 14 sextants unaffected by tumor; in these sextants (10 of which had HGPIN alone), the mean SUVmax was 7.2 ± 3.1 (range, 4.0–12.0).

PET/CT found 108 sextants without evidence of abnormal ^{11}C-choline uptake. These findings were true negative in 59 of the sextants and false negative in 49; in those 49, histologic examination proved the presence of cancer foci.

Of the 59 sextants with true-negative findings, histologic examination showed that 14 had HGPIN (mean SUVmax, 2.0 ± 0.5; range, 1.1 ± 2.8), 4 had acute prostatitis (mean SUVmax, 2.4 ± 0.6; range, 1.8 ± 3.0), and 3 had both HGPIN and acute prostatitis (mean SUVmax, 3.1 ± 0.9; range, 2.3–4.0). In 38, no prostatic disorder was found on histologic examination (mean SUVmax, 2.4 ± 0.6; range, 1.1–4.0) (Table 3).

PET/CT had a sensitivity of 66%, a specificity of 81%, an accuracy of 71%, a positive predictive value of 87%, and a negative predictive value of 55%.

No statistically significant difference between tumors and HGPIN was found with either SUVmax (Fig. 3) or T/B ratio. Mean SUVmax was 6.93 ± 2.93 (range, 4–12) and 5.05 ± 1.86 (range, 2.2–10) for HGPIN and cancer, respectively. The overlap interval (4.0–10.0) included 85% of cancer lesions. Similarly, the mean T/B ratio for HGPIN and cancer foci was 2.16 ± 0.40 (range, 1.4–2.9) and 2.01 ± 0.49 (range, 1.4–3.4), respectively. In this case, the overlap interval included 100% of HGPIN and 90.5% of cancer foci.

We found no statistically significant linear correlation between SUVmax and tumor grade ($R^2 = 0.007$), SUVmax and Gleason score ($R^2 = 0.05$), or SUVmax and PSA ($R^2 = 0.009$).

In 3 patients (patients 12, 34, and 36), the initial prostate biopsy failed to detect prostate cancer because the tumor was located anteriorly in the transition zone: Biopsy repeated on the basis of PET/CT results revealed prostate cancer in the transition zone, and step-section histopathologic examination after radical prostatectomy confirmed the presence of cancer in only this region (Fig. 4).

Four patients had results positive for lymph node metastasis at pathologic evaluation; in 2 of these 4, PET/CT revealed lymph node involvement with clear focal accumulation of ^{11}C-choline (bilateral lymph nodes > 1.5 cm [patient 24] and a lymph node of 2 cm [patient 32]). In 2 patients (patients 16 and 25), PET/CT failed to detect lymphatic involvement, whereas histologic examination showed micrometastases (4 and 7 mm).

In the 5-patient control group, HGPIN was detected in 16 of 30 sextants; ^{11}C-choline PET/CT showed pathologic findings in 5 of 16 sextants in 3 patients (T/B ratio mean value, 1.6; mean SUVmax, 4.1), whereas results were completely negative in 2 patients. Unlike the excellent results of a previous study published by De Jong (*28*), in our study ^{11}C-choline PET/CT succeeded in detecting bladder cancer in only 2 patients (patients 2 and 5, with an SUVmax of, respectively, 8.9 and 6.8). The failure to identify the presence of bladder cancer in the other 3 patients could be due to the presence of urinary radioactivity in 2 patients (patients 1 and 3) and the limited and superficial extension of tumor in the other patient (patient 4).

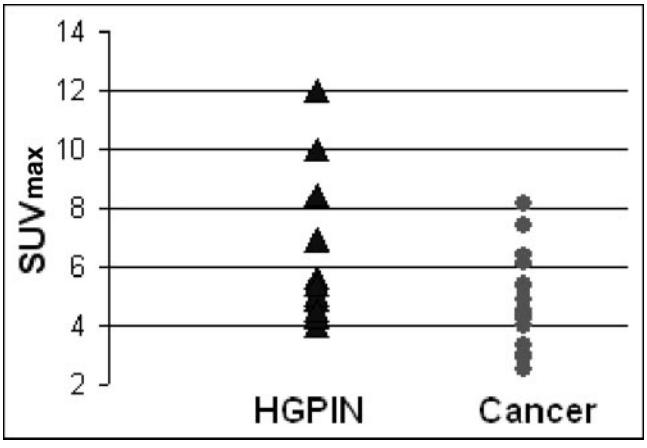

FIGURE 3. Correlation between SUVmax and lesion type.

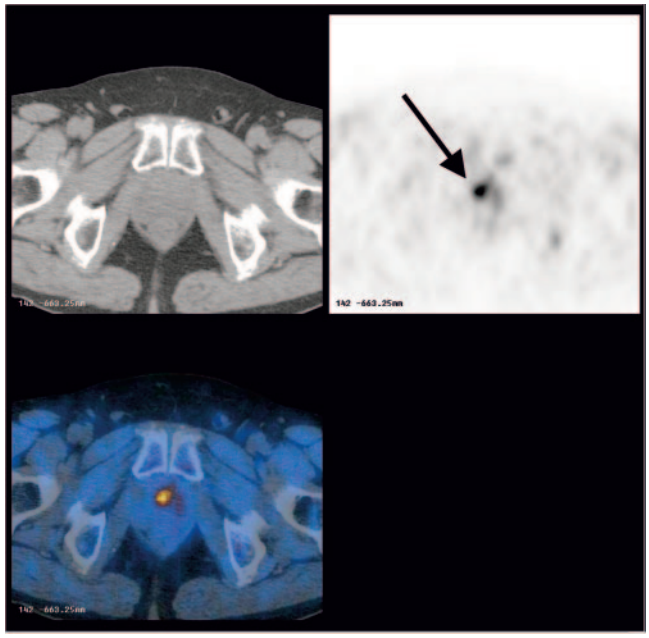

FIGURE 4. Patient 36: Transaxial PET/CT images show 1 focus of pathologic uptake in anterior transitional zone (arrow). First biopsy failed to detect cancer foci, whereas repeated biopsy using PET/CT images detected sites of cancer.

DISCUSSION

The combination of DRE, PSA, and TRUS biopsy is used for the detection of prostate cancer. Because TRUS biopsy often fails to determine the location of prostate cancer, repeated random biopsies are considered by many authors to represent the standard method for prostate cancer detection. However, despite efforts to refine the indication for prostate biopsies by means of PSA-derived indices such as PSA free ratio, PSA density, PSA velocity, and PSA relationship to age, the false-negative biopsy rate remains unacceptably high. An imaging technique able to reveal a suspected area in a certain sextant of the gland would increase the cancer detection rate by enabling additional guided biopsy cores to be obtained.

Recent studies have assessed the role of different positron-emitting tracers for localization and detection of prostate cancer (*12–17*). Reports about the efficacy of ^{11}C-choline in the detection of localized prostate cancer are still rare and show controversial results (*20–22*). However, to our knowledge, no study has correlated PET/CT scan results with whole-prostate histologic confirmation.

This study showed the feasibility of using ^{11}C-choline PET/CT to identify cancer foci. ^{11}C-Choline PET/CT suc-

ceeded in detecting cancer foci in 94 of 143 sextants with histologically proven cancer and failed in 49 of 143 sextants.

Prostate cancer is characterized by multiple foci (in our study, 143 foci in 36 patients), which often are small. The limited spatial resolution of PET/CT scanners is well known, with the scanners unable to detect lesions smaller than 5 mm. In addition, the partial-volume effect could be another cause for failure to detect small lesions. Furthermore, prostate cancer may show a low ^{11}C-choline uptake; in our study, 13 of 93 cancer foci detected with ^{11}C-choline PET/CT had an SUVmax inferior to 3. A faint increase of tracer uptake (i.e., SUVmax < 2.5) is hardly detectable. The wide SUVmax range measured for cancer foci reflects the heterogeneity of prostate cancer, and one could assume that ^{11}C-choline PET/CT fails to detect all cancer foci because of their differences in metabolic state. These 2 conditions (small dimension and low uptake) could explain the high rate of false-negative results with ^{11}C-choline PET/CT.

In our study, the fact that 94 of 108 sextants with a pathologic T/B ratio corresponded to cancer foci with a specificity of 82% indicates that not all hot spots on ^{11}C-choline PET/CT images correspond to a cancer focus: On histologic examination, 10 of 108 foci of ^{11}C-choline uptake were referable to HGPIN, 2 to acute prostatitis, and 2 (detected by PET/CT) to normal tissue or benign prostate hyperplasia. This surprisingly high specificity of ^{11}C-choline PET/CT, however, should be regarded with caution because of the selected patient population. For this study, we only retrospectively enrolled patients with histologically proven prostate cancer.

Although more than half of histologically detected HGPIN foci showed no abnormal ^{11}C-choline uptake (18 of 30 sextants), our study demonstrated that HGPIN can accumulate ^{11}C-choline. To our knowledge, no paper has described an increased uptake of ^{11}C-choline by this pathologic entity. In our series, 5 sextants of the control group and 10 sextants of the patient population with proven HGPIN showed high uptake of ^{11}C-choline. This finding strongly supports the hypothesis that some HGPIN may show pathologic uptake of ^{11}C-choline. Because HGPIN and carcinoma have a strong tendency to be present simultaneously and exhibit the same "zonal" origin and anatomic proximity (*29,30*), a possible explanation for pathologic uptake of ^{11}C-choline in only some HGPIN foci could be that some of these regions harbored a small focus of cancer undetected by pathologists. The complete overlap of SUVmax and T/B ratio between cancer foci and HGPIN foci detected by PET/CT seems to support this hypothesis and points out that no SUVmax or T/B ratio cutoff can help to differentiate between cancer and HGPIN. Another reason for the high ^{11}C-choline uptake of some HGPIN foci could be the different metabolic states of HGPIN lesions.

Malignant prostate tumors localized in an apicoanterior peripheral zone or transition zone are often missed on conventional imaging. Tumors that arise in these areas are often difficult to palpate on DRE or even to sample by TRUS-guided biopsy. In our population, 3 patients with cancer foci localized only in the transition zone produced false-negative results on the first TRUS-guided biopsy, although ^{11}C-choline PET/CT had already shown pathologic uptake in the anterior region of the gland. Biopsy repeated on the basis of PET/CT findings also confirmed cancer foci in the transition zone. One may assume that in a selected patient population with negative findings on the first biopsy but at a high risk of cancer, the use of ^{11}C-choline PET/CT could be helpful as a second-line imaging method. In fact, additional biopsies should be directed at the region of abnormal uptake on PET/CT and at the immediately adjacent areas. Actually, in patients at high risk of prostate cancer, the focus of ^{11}C-choline uptake will more likely correspond to a focus of cancer instead of a benign prostatic disorder. However, further studies are needed to assess the usefulness of ^{11}C-choline PET/CT in clinical practice.

Our study had, however, some limitations. First, the matching process was complicated by differences in technique for 2 principal reasons: The angle at which the histopathologic sections were cut (i.e., perpendicular to the prostate axis) differed from the angle at which imaging was performed (i.e., perpendicular to the body axis), and the size and shape of the prostate could change as a result of tissue shrinkage during fixation.

CONCLUSION

At present, the only indication for the study of prostate cancer with ^{11}C-choline PET/CT is the evaluation of suspected recurrence after first-line treatment. The available data and the small patient population of previous papers do not permit us to judge the true role of this imaging modality in prostate cancer diagnosis. Our study confirms that ^{11}C-choline PET/CT is able to reveal foci of prostate cancer, but further studies are warranted to evaluate the specificity of PET/CT with ^{11}C-choline for identifying prostate tumors. For this reason, our data do not allow us to recommend the routine use of ^{11}C-choline PET/CT as a first-line screening procedure in men at high risk of prostate cancer. A potential application of ^{11}C-choline PET/CT may be to increase the detection rate of cancer on repeated biopsies in patients who have a persistently high risk of prostate cancer and who have undergone multiple, iterative TRUS-guided biopsies with negative findings.

REFERENCES

1. Catalona WJ, Richie JP, Ahmann FR, et al. Comparison of digital rectal examination and serum prostate specific antigen in the early detection of prostate cancer: results of a multicenter clinical trial of 6.630 men. *J Urol.* 1994;15:1283–1290.
2. Polascik TJ, Oesterling JE, Partin AW. Prostate specific antigen: a decade of discovery—what we have learned and where we are going. *J Urol.* 1999;162:293–306.
3. Thompson IM, Pauler DK, Goodman PJ, et al. Prevalence of prostate cancer among men with a prostate-specific antigen level < or =4.0 ng per milliliter. *N Engl J Med.* 2004 27;350:2239–2246.

4. Lujan M, Paez A, Miravalles E. Prostate cancer detection is also relevant in low prostate specific antigen ranges. *Eur Urol.* 2004;45:155–159.
5. Sedelaar JP, Vijverberg PL, De Reijke TM, et al. Transrectal ultrasound in the diagnosis of prostate cancer: state of the art and perspectives. *Eur Urol.* 2001; 40:275–284.
6. Chang JJ, Shinohara K, Bhargava V, et al. Prospective evaluation of lateral biopsies of the peripheral zone for prostate cancer detection. *J Urol.* 1998;160: 2111–2114.
7. Beerlage HP, De Reijke TM, de la Rosette JJ. Considerations regarding prostate biopsies. *Eur Urol.* 1998;34:303–312.
8. Bartolozzi C, Menchi I, Lencioni R, et al. Local staging of prostate carcinoma with endorectal coil MRI: correlation with whole-mount radical prostatectomy specimens. *Eur Radiol.* 1996;6:339–345.
9. White S, Hricak H, Forstner R, et al. Prostate cancer: effect of postbiopsy hemorrhage on interpretation of MR images. *Radiology.* 1995;195:385–390.
10. Wefer AE, Hricak H, Vigneron DB, et al. Sextant localisation of prostate cancer: comparison of sextant biopsy, magnetic resonance imaging and magnetic resonance spectroscopic imaging with step section histology. *J Urol.* 2000;164:400–404.
11. Coakley F, Qayyum A, Kurhanewicz J. Magnetic resonance imaging and spectroscopic imaging of prostate cancer. *J Urol.* 2003;170(suppl):S69–S76.
12. Effert PJ, Bares R, Handt S, et al. Metabolic imaging of untreated prostate cancer by positron emission tomography with 18 fluorine-labeled deoxyglucose. *J Urol.* 1996;155:994–998.
13. Liu IJ, Zafar MB, Lai YH, et al. Fluorodeoxyglucose positron emission tomography studies in diagnosis and staging of clinically organ-confined prostate cancer. *Urology.* 2001;57:108–111.
14. Kato T, Tsukamoto E, Kuge Y, et al. Accumulation of [^{11}C]acetate in normal prostate and benign prostatic hyperplasia: comparison with prostate cancer. *Eur J Nucl Med.* 2002;29:1492–1495.
15. Oyama N, Akino H, Kanamaru H, et al. [^{11}C]acetate PET imaging of prostate cancer. *J Nucl Med.* 2002;43:181–186.
16. Gyorgy T, Zsolt L, Laszlo B, et al. Detection of prostate cancer with ^{11}C-methionine positron emission tomography. *J Urol.* 2005;173:66–69.
17. Kwee SA, Coel MN, Lim J, et al. Prostate cancer localization with 18fluorine fluorocholine positron emission tomography. *J Urol.* 2005;173:252–255.
18. Hara T, Kosaka N, Kishi H. PET imaging of prostate cancer using carbon-11-choline. *J Nucl Med.* 1998;39:990–995.
19. Kotzerke J, Prang J, Neumaier B, et al. Experience with carbon-11 choline positron emission tomography in prostate carcinoma. *Eur J Nucl Med.* 2000;27: 1415–1419.
20. Sutinen E, Nurmi M, Roivainen A, et al. Kinetics of [^{11}C] choline uptake in prostate cancer: a PET study. *Eur J Nucl Med Mol Imaging.* 2003;31:317–324.
21. De Jong IJ, Pruim J, Elsinga PH, et al. Visualization of prostate cancer with ^{11}C-choline positron emission tomography. *Eur Urol.* 2002;42:18–23.
22. Yoshida S, Nakagomi K, Goto S, et al. C-Choline positron emission tomography in prostate cancer: primary staging and recurrent site staging. *Urol Int.* 2005;74: 214–220.
23. Breeuwsma AJ, Pruim J, Jongen MM, et al. In vivo uptake of [^{11}C]choline does not correlate with cell proliferation in human prostate cancer. *Eur J Nucl Med Mol Imaging.* 2005;32:668–673.
24. Gore JL, Shariat SF, Miles BJ, et al. Optimal combinations of systematic sextant and laterally directed biopsies for the detection of prostate cancer. *J Urol.* 2001;165:1554–1559.
25. Pascali C, Bogni A, Iwata R, et al. ^{11}C-Methylation on C18 SepPak cartridge: a convenient way to produce [N-methyl-^{11}C] choline. *J Labelled Compds Radiopharm.* 2000;49:195–203.
26. Townsend DW, Beyer T. A combined PET/CT scanner: the path to true image fusion. *Br J Radiol.* 2002;75:S24–S30.
27. Bar-Shalom R, Yefremov N, Guralnik L, et al. Clinical performance of PET/CT in evaluation of cancer: additional value for diagnostic imaging and patient management. *J Nucl Med.* 2003;44:1200–1209.
28. De Jong IJ, Pruim J, Elsinga PH, et al. Visualization of bladder cancer using ^{11}C-choline PET: first clinical experience. *Eur J Nucl Med.* 2002;29:1283–1288.
29. Sakr WA, Grignon DJ. Prostatic intraepithelial neoplasia and atypical adenomatous hyperplasia: relationship to pathologic parameters, volume and spatial distribution of carcinoma of the prostate. *Anal Quant Cytol Histol.* 1998;20:417–423.
30. Bostwick DG, Qian J. High-grade prostatic intraepithelial neoplasia. *Mod Pathol.* 2004;17:360–379.

JNM The Journal of NUCLEAR MEDICINE

Detection and Localization of Prostate Cancer: Correlation of ^{11}C-Choline PET/CT with Histopathologic Step-Section Analysis

Mohsen Farsad, Riccardo Schiavina, Paolo Castellucci, Cristina Nanni, Barbara Corti, Giuseppe Martorana, Romeo Canini, Walter Grigioni, Stefano Boschi, Mario Marengo, Cinzia Pettinato, Eugenio Salizzoni, Nino Monetti, Roberto Franchi and Stefano Fanti

J Nucl Med. 2005;46:1642-1649.

The Journal of Nuclear Medicine is published monthly.
SNMMI | Society of Nuclear Medicine and Molecular Imaging
1850 Samuel Morse Drive, Reston, VA 20190.
(Print ISSN: 0161-5505, Online ISSN: 2159-662X)

SNMMI SOCIETY OF NUCLEAR MEDICINE AND MOLECULAR IMAGING